2018

Axial Compressive Behavior of Steel Equal Angle Section-Reinforced Square High-Strength Concrete Column

Ayoob Ibrahim
University of Wollongong, aaii884@uowmail.edu.au

M Neaz Sheikh
University of Wollongong, msheikh@uow.edu.au

Muhammad N. S Hadi
University of Wollongong, mhadi@uow.edu.au

Axial Compressive Behavior of Steel Equal Angle Section-Reinforced Square High-Strength Concrete Column

Abstract

A new method of reinforcing concrete columns with steel equal angle (SEA) sections has been investigated. A total of 12 square high-strength concrete (HSC) column specimens (with 210 mm [8.26 in.] sides and 600 mm [23.62 in.] height) reinforced longitudinally with either steel bars or SEA sections were cast and tested. The lateral tie spacing of specimens varied from 50 to 400 mm (1.96 to 15.74 in.). The influences of the type of longitudinal reinforcement and the spacing of lateral ties on the behavior of HSC specimens under axial compression were investigated. Experimental results showed that the use of the SEA sections as longitudinal reinforcements in HSC column specimens led to significant improvements in the axial load-carrying capacity and ductility compared to the corresponding HSC column specimens reinforced longitudinally with steel bars.

Publication Details

Ibrahim, A. A., Sheikh, M. & Hadi, M. N. S. (2018). Axial Compressive Behavior of Steel Equal Angle Section-Reinforced Square High-Strength Concrete Column. Aci Structural Journal, 115 (5), 1431-1442.

AXIAL COMPRESSIVE BEHAVIOR OF SEA SECTION REINFORCED SQUARE HSC COLUMN

by Ayoob A. Ibrahim, M. Neaz Sheikh, Muhammad N. S. Hadi

Biography:

Ayoob A. Ibrahim is a PhD candidate in the School of Civil, Mining & Environmental Engineering University of Wollongong, Australia. He received his BS from University of Babylon, Iraq, in 2002 and MS from University of Babylon, in 2005. His research interests include steel fiber reinforced concrete and members under cyclic loading.

M. Neaz Sheikh is an Associate Professor in the School of Civil, Mining & Environmental Engineering, University of Wollongong, Australia. He received his BSc (Civil Engineering) from Chittagong University of Engineering and Technology (CUET), Bangladesh, and his MPhil and PhD from the University of Hong Kong, China. His research interests include earthquake engineering, concrete structures, and application of advanced composite materials in civil infrastructure.

ACI member **Muhammad N. S. Hadi** is an Associate Professor in the School of Civil, Mining & Environmental Engineering, University of Wollongong, Australia. He received his BS and MS from the University of Baghdad, Iraq, in 1977 and 1980, respectively, and his PhD from the University of Leeds, UK, in 1989. His research interests include analysis and design of concrete structures.

ABSTRACT

A new method of reinforcing concrete columns with steel equal angle (SEA) sections has been investigated. A total of 12 square High Strength Concrete (HSC) column specimens (210 mm (8.26 in.) sides and 600 mm (23.62 in.) height) reinforced longitudinally with either steel bars or SEA sections were cast and tested. The lateral tie spacing of specimens varied from 50 mm (1.96 in.) to 400 mm (15.74 in.). The influences of the type of longitudinal reinforcement and the spacing of lateral ties on the behavior of HSC specimens under axial compression were investigated.

Experimental results showed that the use of the SEA sections as longitudinal reinforcements in HSC column specimens led to significant improvements in the axial load carrying capacity and ductility compared to the corresponding HSC column specimens reinforced longitudinally with steel bars.

Keywords: Reinforced concrete; Columns; Steel Equal Angle; Tie spacing; Axial load; Buckling; Ductility.

INTRODUCTION

Composite columns are usually used in high-rise buildings due to high strength, stiffness, ductility, and seismic resistance of composite columns.[1,2] There are two main types of composite columns: concrete encased steel section and concrete filled hollow steel section. Encased composite columns (concrete encased steel section) are being increasingly used as structural members because of their higher fire resistance compared to the concrete filled hollow steel sections, which require protection against fire.[3] Also, in the encased composite column, the local buckling resistance of encased steel section is higher.[4] In addition, the use of encased steel sections in composite columns reduces the cross-sectional dimensions and increases the strength-to-weight ratio of the columns.[2] According to a detailed literature review carried out herein, no study is available in the literature that deals with high strength concrete (HSC) columns reinforced with steel equal angle (SEA) sections.

The use of high-strength concrete (HSC) in the buildings has increased in recent years.[5-7] However, the ductility of HSC is lower than the ductility of normal strength concrete (NSC).[8-11] Also, HSC columns under concentric axial compression experience premature concrete cover spalling, which considerably decreases the axial strength of columns.[12] Therefore, the ductility and the strength of HSC columns were extensively investigated.[13-15] In general, more lateral reinforcement is required in HSC columns than in NSC columns to achieve a similar ductility.[16,17]

Concrete columns are commonly reinforced longitudinally with conventional steel bars and laterally with either ties or helices. For square concrete columns reinforced with lateral ties, the area of the

effectively confined concrete core is less than the total area of the concrete core, which results in lower strength and ductility of the square RC columns.[18] In this study, Steel Equal Angle (SEA) sections were used as longitudinal reinforcement for square HSC columns. The SEA sections have been widely used in the construction of steel structures. [19-21] However, no previous study investigated the use of SEA sections in reinforcing HSC columns. The use of SEA sections instead of conventional steel bars in the square HSC columns can increase the confinement of the concrete core, which may increase the ductility of columns under axial compression. In addition, the SEA section has a higher second moment of area than the conventional steel bar for the same cross-sectional area, which may increase the buckling load of the longitudinal reinforcement. As a result, less lateral ties may be required in HSC columns reinforced with SEA sections than in HSC columns reinforced with steel bars. This study investigates the influence of the SEA sections on the failure modes, maximum axial load, confinement efficiency and post-peak axial load-axial deformation behavior of the square HSC columns.

RESEARCH SIGNIFIANCE

One of the main problems associated with the use of HSC in the construction of reinforced concrete columns is that the ductility of HSC columns is usually lower than the ductility of NSC columns. To increase the ductility of HSC columns under axial compression, this study investigates the effectiveness of the use of SEA sections, instead of steel bars, as longitudinal reinforcements in square HSC columns. The findings of this study can be used to evaluate the feasibility of reinforcing square HSC columns with longitudinal SEA sections.

EXPERIMENTAL PROGRAM

Specimen Details

The experimental program aimed at investigating the influence of the longitudinal reinforcement (steel bars and SEA sections) and the spacing of lateral reinforcement (ties) on the behavior of square

HSC column specimens under axial compression. A total of 12 square HSC column specimens with 210 mm × 210 mm (8.26 in. × 8.26 in.) cross-section and 600 mm (23.62 in.) height were cast and tested under concentric axial compression. The tested specimens were divided into three groups of four specimens (**Table 1**). The tie spacing in each group of specimens varied from 50 mm (1.96 in.) to 400 mm (15.74 in.) (**Fig. 1**). The specimens in the first group (Group B) served as the reference specimens and were reinforced longitudinally with four N12 steel bars (12 mm (0.47 in.) diameter deformed steel bars with 500 MPa (72.51 ksi) nominal yield tensile strength) and laterally with R10 steel bars (10 mm (0.39 in.) diameter plain steel bars with 250 MPa (36.25 ksi) nominal yield tensile strength). In the second group (Group A30), the specimens were reinforced longitudinally with four A30 SEA sections (29.1 mm (1.14 in.) leg width and 2.25 mm (0.08 in.) thickness with 350 MPa (50.76 ksi) nominal yield tensile strength) and laterally with R10 steel bars. The specimens in the third group (Group A40) were reinforced longitudinally with four A40 SEA sections (39.3 mm (1.54 in.) leg width and 3.7 mm (0.14 in.) thickness with 450 MPa (65.27 ksi) nominal yield tensile strength) and laterally with R10 steel bars.

The tested column specimens were identified in two parts (**Table 1**). In the first part, B, A30, and A40 represent N12 steel bar, A30 SEA section and A40 SEA section, respectively. In the second part S50, S100, S200, and S400 represent the tie spacing of 50 mm (1.96 in.), 100 mm (3.93 in.), 200 mm (7.87 in.) and 400 mm (15.74 in.) at centers, respectively. For instance, Specimen A30-S100 was reinforced longitudinally with four A30 SEA sections and laterally with R10 steel bars having a tie spacing of 100 mm (3.93 in.) at centers.

Material Properties

The column specimens were cast vertically with ready-mix high strength concrete (HSC) provided by a local supplier. The maximum size of the coarse aggregate was 10 mm. The slump of the concrete, tested according to AS 1012.3.1-14,[22] was 180 mm, which represented a good workability

of the concrete. The compressive strength of the concrete was determined by testing three concrete cylinder specimens of 100 mm (3.93 in.) diameter and 200 mm (7.87 in.) height according to AS 1012.9-99.[23] The average 28-day compressive strength of the concrete was 68.5 MPa (9.93 ksi). Three samples from each of N12 bars and R10 bars were tested in tension according to AS 1391-07[24] by using 500 kN (112.40 kip) Instron testing machine in the Structural Engineering Laboratory at the University of Wollongong, Australia. The average yield tensile strengths of N12 and R10 steel bars were 556 MPa (80.64 ksi) and 323 MPa (46.84 ksi), respectively.

Two different steel equal angle (SEA) sections were used in this study. The SEA sections were supplied by OneSteel.[25] The nominal and measured dimensions of the SEA sections are reported in **Table 2**. For each SEA section, tensile coupon specimens were taken from the flat portion of the SEA section. Three samples from each of A30 and A40 SEA sections were tested according to AS 1391-07[24] by using 500 kN (112.40 kip) Instron testing machine. The average yield tensile strengths of A30 and A40 SEA sections were 374 MPa (54.24 ksi) and 473 MPa (68.60 ksi), respectively.

Formwork and Steel Cages

The formwork used for casting the concrete specimens was fabricated from 17 mm (0.66 in.) thick plywood. The formwork included two groups of small formwork. Each group was used for casting six specimens. The small formwork was fabricated using two large sheets of plywood (1439 mm (56.65 in.) × 600 mm (23.62 in.) × 17 mm (0.66 in.)) and seven small sheets of plywood (220 mm (8.66 in.) × 600 mm (23.62 in.) × 17 mm (0.66 in.)). The formwork was prepared by placing the plywood sheets together with screws. The longitudinal N12 steel bars and SEA sections were cut into a length of 560 mm (22.04 in.) to maintain a 20 mm (0.78 in.) concrete clear cover at the top and the bottom of the specimens. For all specimens, the concrete side cover was 21 mm (0.82 in.). Square ties were fabricated from R10 steel bars for all specimens. All ties were bent at four corners with a radius of 6 mm (0.23 in.) so that the ties could be placed over the SEA sections. Also, the ties were bent for 90-degree hooks around one of the longitudinal reinforcement and extended for an overlap of 80 mm (3.14 in.) at both ends. Each tie was welded at three points on the overlap. The

spacing of lateral ties was reduced to 40 mm (1.57 in.) at the end regions to prevent premature failures at the ends (**Fig. 1**).

Deformed N12 steel bars and smooth SEA sections were used as longitudinal reinforcement. In order to decrease the possible slippage of the SEA sections in the specimens reinforced with SEA sections, two short plain steel bars (8 mm (0.31 in.) diameter and 40 mm (1.57 in.) long) were welded laterally between the ends of the SEA sections at the top and the bottom. In addition, two short steel bars (16 mm (0.62 in.) diameter and 70 mm (2.75 in.) length) were welded internally and axially at the top and bottom of each SEA section (**Fig. 2**). Afterwards, all steel cages were prepared by placing the longitudinal and lateral reinforcement together with steel wires. The concrete was poured into the formwork in three levels. An electric vibrator was used at every level to compact the concrete and remove air bubbles. After 24 hours, the specimens were covered with wet hessian for 28 days to ensure that the specimens remained under moist conditions. The specimens were removed from the formwork after 14 days from casting and kept covered with wet hessian until 28 days from casting.

Instrumentation and Testing Procedure

The column specimens were instrumented externally to capture the axial deformation of the specimens by using two linear variable differential transducers (LVDTs), as shown in **Fig. 3**. The LVDTs were attached to the heads of the testing machine at two opposite corners to capture the axial deformation of the specimens (**Fig. 3**). The axial compression was captured by the internal load cell of the testing machine.

To ensure that the load is applied uniformly, the top surface (rough surface) of the column specimens was capped with a thin layer of high strength plaster. To avoid premature failure of the specimens during testing, the top and the bottom ends of the column specimens were wrapped by two layers of Carbon Fiber Reinforced Polymer (CFRP) sheets with a width of 90 mm (3.54 in.). The testing of the column specimens was carried out using the 5000 kN (1124.04 kip) Denison compression testing machine in the Structural Engineering Laboratories at the University of Wollongong, Australia. At the beginning of the test, each specimen was preloaded to about 10% of the expected maximum axial

load of the specimens to prevent any movement in the specimens at the beginning of the test. Afterwards, the test resumed under a displacement controlled concentric axial loading at the rate of 0.3 mm/minute (0.01 in./minute) until the strength of the specimens dropped to about 20% of the maximum axial load. The LVDTs were connected to a data logger to record the data at every two seconds.

EXPERIMENTAL RESULTS AND DISCUSSIONS

Definition of Ductility

The ductility (μ) of the tested column specimens was calculated based on the energy absorption capacity of the specimen. The ductility was calculated as the ratio of the area under the axial load-axial deformation curve up to the ultimate deformation and the area up to the deformation corresponding to the yield axial load.[26,27]

$$\mu = \frac{A_u}{A_y} \quad (1)$$

where A_y and A_u are the areas under the axial load-axial deformation curves up to the yield deformation (Δ_y) and up to the ultimate deformation (Δ_u), respectively. The yield deformation (Δ_y) is taken as the axial deformation corresponding to the intersection point of an extension line through 75% of the maximum axial load and the horizontal line from the maximum axial load.[28] The ultimate deformation was measured as the axial deformation at an axial load equal to 80% of the maximum axial load in the descending branch of the axial load-axial deformation curve.[29]

Behavior of Column Specimens with 50 mm Tie Spacing

Specimens B-S50, A30-S50, and A40-S50 were reinforced longitudinally with N12 steel bars, A30 SEA sections and A40 SEA sections, respectively. The spacing of lateral ties for B-S50, A30-S50, and A40-S50 was 50 mm at centers (center-to-center). All the specimens were tested up to about 20% of the maximum axial load in the post-peak descending branch of the axial load-axial deformation response. The maximum axial load and corresponding axial deformation of the

Specimens B-S50, A30-S50 and A40-S50 are reported in **Table 3**. The maximum axial load represents the axial load carried by the gross concrete cross-sectional area (concrete core and concrete cover) of specimens. Generally, there were some visual cracks prior to the maximum axial load. The first hairline cracks in Specimens B-S50 and A30-S50 appeared at about 88% and 86%, respectively, of the corresponding maximum axial loads. These hairline cracks were observed at the mid-height of the specimens. As the axial load increased, the number, length, and width of the cracks increased until the spalling of the concrete cover. The first hairline crack in Specimen A40-S50 was initiated at approximately 90% of the maximum axial load. This crack occurred at the top one-third height of the specimen and then the cracks appeared at the midheight of the specimen. Afterwards, the number, length and width of the cracks increased until the spalling of the concrete cover. The failure of Specimens B-S50, A30-S50, and A40-S50 was attributed to the spalling of large pieces of the concrete cover, which was followed by outward buckling of longitudinal reinforcement and fracture of lateral ties at welded points, as shown in **Fig. 4**.

The axial load-axial deformation responses of the specimens with 50 mm tie spacing are shown in **Fig. 5(a).** The maximum axial load carried by the reference Specimen B-S50 was 2929 kN (658.46 kip), which is about 11.6% higher than the maximum axial load of Specimens A30-S50. The maximum axial load of Specimen B-S50 was higher because the average yield tensile strength of N12 steel bars was 49% higher than the average yield tensile strength of A30 SEA sections. At the maximum axial loads, the force contribution of N12 steel bars in Specimen B-S50 was 27% greater than the force contribution of A30 SEA sections in Specimen A30-S50. However, the ductility of Specimen A30-S50 was 44.4% greater than the ductility of Specimen B-S50. The greater ductility of Specimen A30-S50 indicates that SEA sections increased the area of the effectively confined concrete core after cracking occurred at the cover-core interface. The maximum axial load of Specimens A40-S50 was 2.7% higher than the maximum axial load of Specimen B-S50. Also, the ductility of Specimen A40-S50 was 50.0% higher than the ductility of Specimen B-S50. The reason for the higher maximum axial load and the ductility was attributed to the higher confinement to the

concrete core provided by the A40 SEA sections. Another possible reason was that at the maximum axial load, the force contribution of A40 SEA in Specimen A40-S50 was about 50% higher than the force contribution of N12 steel bars in Specimen B-S50. The maximum axial load of Specimen A40-S50 was 14.6% higher than the maximum axial load of Specimen A30-S50. The reason for the higher maximum axial load was that at the maximum axial load, the force contribution of A40 SEA in Specimen A40-S50 was about 64% higher than the force contribution of A30 SEA sections in Specimen A30-S50. Also, Specimen A40-S50 achieved only 3.8% higher ductility than Specimen A30-S50. The higher ductility for Specimen A40-S50 indicates that the A40 SEA sections were more effective than the A30 SEA sections in confining the concrete core of the specimen.

Behavior of Column Specimens with 100 mm Tie Spacing

Specimens B-S100, A30-S100, and A40-S100 were reinforced longitudinally with N12 steel bars, A30 SEA sections, and A40 SEA sections, respectively. The spacing of lateral ties for B-S100, A30-S100, and A40-S100 was 100 mm (3.93 in.) at centers. All the specimens were tested up to about 20% of the maximum axial load in the post-peak descending branch of the axial load-axial deformation response. The test results of Specimens B-S100, A30-S100, and A40-S100 are reported in **Table 3**. The first hairline cracks in Specimens B-S100 and A30-S100 appeared at approximately 90% and 82%, respectively, of the corresponding maximum axial loads. The cracks occurred at the top one-third height of the specimens and then the cracks were observed at the midheight of the specimens. Afterwards, the number, length, and width of cracks continued to increase until the concrete cover spalled off. The hairline crack in Specimen A40-S100 was initiated at about 83% of the maximum axial load. These cracks were observed at the top one-third of the specimen and then the cracks extended downwards and continued to increase in number and size until the spalling of the concrete cover occurred. The failure of Specimens B-S100, A30-S100, and A40-S100 was characterized by the spalling of concrete cover, which was followed by outward buckling of longitudinal reinforcement (**Fig. 4**).

The axial load-axial deformation responses of the specimens with 100 mm tie spacing are shown in **Fig. 5(b)**. The maximum axial load of Specimen B-S100 was similar to the maximum axial load of Specimen A30-S100, although, at maximum axial loads, the force contribution of N12 steel bars in Specimen B-S100 was 27% higher than the force contribution of A30 SEA sections in Specimen A30-S100. It was also observed that the ductility of Specimen A30-S100 was 12.5% higher than the ductility of the Specimen B-S100. Specimen A40-S100 obtained 8.0% higher maximum axial load compared to Specimen B-S100. The reason for the higher maximum axial load was that at the maximum axial load, the force contribution of A40 SEA sections in Specimen A40-S100 was about 50% greater than the force contribution of N12 steel bars in Specimen B-S100. In addition, Specimen A40-S100 achieved 18.8% higher ductility than Specimen B-S100. The use of SEA sections as longitudinal reinforcement resulted in higher ductility compared to the conventional steel bar reinforced specimens due to the increased confinement of the concrete core provided by the SEA sections. It is noted that specimens reinforced longitudinally with N12 steel bars had about 30% and 50% lower confinement effectiveness coefficient (k_e) than specimens reinforced longitudinally with A30 and A40 SEA sections, respectively. The confinement effectiveness coefficient (k_e) of the specimens was calculated based on Mander et al. [30] The maximum axial load of Specimen A40-S100 was 8.3% higher than the maximum axial load of Specimen A30-S100. Also, Specimen A40-S100 achieved 5.6% higher ductility compared to Specimen A30-S100. This may be because the force contribution of A40 SEA in Specimen A40-S100 was about 64% greater than the force contribution of A30 SEA sections in Specimen A30-S100.

Behavior of Column Specimens with 200 mm Tie Spacing

Specimens B-S200, A30-S200, and A40-S200 were reinforced longitudinally with N12 bars, A30 SEA sections, and A40 SEA sections, respectively. The spacing of lateral ties for Specimens B-S200, A30-S200, and A40-S200 was 200 mm (7.87 in.) at centers. All these specimens were tested up to about 20% of the maximum axial load in the post-peak descending branch of the axial load-axial deformation response. The test results of Specimens B-S200, A30-S200 and A40-S200 are reported

in **Table 3**. For Specimen B-S200, the first hairline crack began at about 93% of the maximum axial load. This first crack occurred at the top one-third height of the specimens and then the cracks appeared at the midheight of the specimen. As the axial load increased close to the failure condition, the number and size of the cracks increased until spalling of the concrete cover was observed. Whereas, the first hairline cracks in Specimens A30-S200 and A40-S200 started at about 91% and 87%, respectively, of the corresponding maximum axial loads. These cracks were observed at the mid-height of the specimens. Afterwards, with the increase of the applied axial load, the number and size of the cracks increased and the concrete cover spalled off. The observed failure in Specimens B-S200 was attributed to the crushing of the concrete core due to the spalling of concrete cover and the instability of longitudinal reinforcements (**Fig. 6**). The failure of Specimens A30-S200 and A40-S200 was attributed to the spalling of the concrete cover, which was followed by outward buckling of longitudinal SEA sections (**Fig. 6**).

The axial load-axial deformation responses of the specimens with 200 mm tie spacing are shown in **Fig. 5(c).** The maximum axial load of Specimen A30-S200 was 2.9% higher than the maximum axial load of Specimen B-S200. It is noted that the average yield tensile strength of steel bars was 49% higher than the average yield tensile strength of A30 SEA sections which resulted in 27% higher force contribution of N12 steel bars in B-S200 specimen compared to the force contribution of A30 SEA section in A30-S200 specimen at the maximum axial load. This increase in the maximum axial load in Specimen A30-S200 was because when the spacing of lateral ties increased, the failure of longitudinal reinforcement (steel bars or SEA sections) tended to be controlled by the buckling more than the yielding of longitudinal reinforcement. The confinement provided by the lateral ties decreased with the increase in the spacing of lateral ties. The maximum axial load of Specimen A30-S200 was higher because A30 SEA section had a higher second moment of area and hence showed higher buckling load. In addition, Specimen A30-S200 obtained 6.7% greater ductility compared to Specimen B-S200. The reason of greater ductility in Specimen A30-S200 was that as the buckling load of longitudinal reinforcement increased, the confinement effect to the concrete core increased.[31]

283 The maximum axial load of Specimen A40-S200 was 16.3% greater than the maximum axial load
284 of Specimen B-S200. The reason of higher maximum axial load might be because the N12 steel bars
285 in Specimen B-S200 buckled before yielding, whereas the A40 SEA sections yielded before buckling
286 due to higher buckling load of A40 SEA sections than the buckling load of N12 steel bars. Also,
287 Specimen A40-S200 showed 13.3% higher ductility than Specimen B-S200. Hence, reinforcing
288 specimens with SEA sections improved the performance of the specimens because of higher buckling
289 load of SEA sections than the buckling load of steel bars and also because of the increase in the
290 effective confinement of concrete core. The higher buckling load for SEA sections was because the
291 second moment of area of the SEA section was greater than the second moment of area of the steel
292 bar for the similar cross-sectional area. Specimen A40-S200 showed only 13.0% higher maximum
293 axial load compared to Specimen A30-S200. The higher maximum axial load in Specimen A40-S200
294 may be because A40 SEA sections in Specimens A40-S200 had higher force contribution than A30
295 SEA sections in Specimen A30-S200. Also, the ductility of Specimen A40-S200 was 6.2% higher
296 than the ductility of Specimen A30-S200. The higher ductility in Specimen A40-S200 indicated that
297 A40 SEA sections provided better confinement of the concrete core.

298 **Behavior of Column Specimens with 400 mm Tie Spacing**

299 Specimens B-S400, A30-S400, and A40-S400 were reinforced longitudinally with N12 steel bars,
300 A30 SEA sections, and A40SEA sections, respectively. The spacing of lateral ties for B-S400, A30-
301 S400, and A40-S400 was 400 mm (15.74 in.) at centers. The test results of Specimens B-S400, A30-
302 S400 and A40-S400 are presented in **Table 3**. It is noted that the spacing of lateral ties in the
303 specimen B-S400 was higher than the required spacing of lateral ties recommended in AS 3600-09[32]
304 and ACI 318-14.[33] Specimen B-S400 was designed to compare the behavior of Specimens A30-S400
305 and A40-S400 in terms of failure mode, strength, and ductility. The first hairline cracks in Specimens
306 B-S400, A30-S400 and A40-S400 started at approximately 90%, 89%, and 88%, respectively, of
307 their maximum axial loads. These cracks were observed at the mid-height of the specimens. As the
308 applied axial load increased close to the maximum axial load, the cracks extended both upwards and

downwards of the specimens. Afterwards, the number and size of the cracks increased and the concrete cover spalled off. The failure in Specimen B-S400 was characterized by the crushing of concrete core, which occurred after the spalling of the concrete cover and outward buckling of longitudinal steel bars (**Fig. 6**). The failure in Specimens A30-S400 and A40-S400 was characterized by outward buckling of longitudinal SEA sections without crushing of concrete core (**Fig. 6**).

The axial load-axial deformation responses of the specimens with 400 mm tie spacing are shown in **Fig. 5(d)**. The maximum axial load of Specimens A30-S400 was 42.5% higher than the maximum axial load of Specimen B-S400. This may be because the use of SEA sections instead of steel bars in reinforcing square HSC column specimens significantly increased the buckling load of longitudinal reinforcement. The minimum second moment of area of the A30 SEA section was about 77% higher than the second moment of the area of the conventional steel bar for the same cross-sectional area. In addition, the minimum radius of gyration of the A30 SEA section was about 50% greater than the radius of gyration of the conventional steel bar for the same cross-sectional area.

The lower axial load carrying capacity of Specimen B-S400 was due to the instability of longitudinal bars (buckling of longitudinal steel bars at an early stage of loading), which pushed out the concrete cover and created weakness planes between the concrete cover and the concrete core. Similar observations were also reported Saatcioglu and Razvi.[34] Therefore, the ductility of Specimen B-S400 was not further analysed. The maximum axial load of Specimen A40-S400 was 52.2% higher than the maximum axial load of Specimen B-S400. This significantly high maximum axial load in Specimen A40-S400 was because the confinement efficiency of the concrete core of the specimens increased by using A40 SEA sections as longitudinal reinforcement instead of N12 steel bars. Another possible reason is that at maximum axial load, the conventional steel bars in Specimen B-S400 reached buckling before yielding of the longitudinal steel bars. However, at maximum axial load, the A40 SEA sections in Specimen A40-S400 yielded before buckling as A40 SEA sections had much higher buckling load than N12 steel bars. The maximum axial load of Specimen A40-S400 was 6.9% higher than the maximum axial load of Specimen A30-S400. Also, the ductility of

335 Specimen A40-S400 was 6.7% higher than the ductility of Specimen A30-S400. This indicates that
336 A40 SEA sections were more effective than A30 SEA sections in confining the concrete core of the
337 specimen.
338
339 **INFLUENCE OF LATERAL TIE SPACING ON THE BEHAVIOR OF THE TESTED**
340 **SPECIMENS**
341 In this section, the influence of increasing the spacing of lateral ties from 50 mm (1.96 in.) to 400
342 mm (15.74 in.) in each group of specimens was investigated and discussed. The main aim is to
343 investigate the effect of increasing lateral tie spacing on the strength, ductility and buckling load for
344 each group of specimens. As discussed above, the use of SEA section as longitudinal reinforcement
345 led to increased effective confinement of the concrete core and greater buckling load compared to
346 the use of the N12 steel bars. Therefore, the improvements in the effective confinement of concrete
347 core and buckling load for SEA sections influenced the strength and ductility of the specimens
348 particularly with the increase in the lateral tie spacing. To be on the safe side, the minimum second
349 moment of area and the minimum radius of gyration of the A30 and A40 SEA sections were selected
350 to compare with the second moment of area and radius of gyration of N12 steel bars. The second
351 moment of area and radius of gyration of N12 steel bar were about 1018 mm^4 (0.0024 in^4) and 3 mm
352 (0.11 in.), respectively. The minimum second moment of area and the minimum radius of gyration
353 of A30 SEA section were about 4380 mm^4 (0.0105 in^4) and 6 mm (0.23 in.). The minimum second
354 moment of area and minimum radius of gyration of A40 SEA section were about 15700 mm^4 (0.0377
355 in^4) and 8 mm (0.31 in.), respectively.
356 The test results of the specimens in Group B are reported in **Table 3**. The axial load-axial deformation
357 responses of the specimens in Group B are presented in **Fig. 7(a)**. The maximum axial load of
358 Specimen B-S50 was 11.5% higher than the maximum axial load of Specimen B-S100. The ductility
359 of Specimen B-S50 was 12.5% greater than the ductility of Specimen B-S100. Specimen B-S50
360 achieved 22.1% and 20.0% higher maximum axial load and ductility, respectively, compared to

Specimen B-S200. Furthermore, the maximum axial load of Specimen B-S50 was 70.6% higher than the maximum axial load of Specimen B-S400. The sharp decrease of the axial load of Specimen B-S400 indicates that the buckling load of longitudinal steel bars and the confinement of the concrete core significantly decreased as the spacing of lateral ties increased from 50 mm (1.96 in.) to 400 mm (15.74 in.). Also, the ductility of the specimen with 400 mm (15.74 in.) tie spacing, which exceeds the required spacing of lateral ties by ACI 318-14,[33] was not calculated as the specimen failed prematurely. The premature failure of Specimen B-S400 was because the large lateral tie spacing of Specimen B-S400 resulted in buckling of the longitudinal reinforcement at an early stage of loading. The test results of the specimens in Group A30 are reported in **Table 3**. The axial load-axial deformation responses of the specimens in Group A30 are presented in **Fig. 7(b)**. Compared to Specimen A30-S100, the maximum axial load of Specimen A30-S50 was only 0.2% higher. This may be because the formation of a natural separation plane between the cover and the concrete core caused the failure of concrete cover in Specimen A30-S50 due to the closely spaced lateral ties. However, Specimen A30-S50 achieved 44.4% higher ductility than Specimen A30-S100. Specimen A30-S50 obtained 6.3% higher maximum axial load than Specimen A30-S200. In addition, the ductility of Specimen A30-S50 was 62.5% higher than the ductility of Specimen A30-S200. Specimen A30-S50 achieved 7.3% and 73.3% higher maximum axial load and ductility, respectively, than Specimen A30-S400. It is noted that the lateral tie spacing of Specimen A30-S50 was 50 mm (1.96 in.) and lateral tie spacing of Specimen A30-S400 was 400 mm (15.74 in.).

The test results of the specimens in Group A40 are reported in **Table 3**. The axial load-axial deformation responses of the specimens in Group A40 are presented in **Fig. 7(c)**. The maximum axial load of Specimen A40-S50 was 6.1% greater than the maximum axial load of Specimen A40-S100. Moreover, the ductility of Specimen A40-S50 was 42.1% higher than the ductility of Specimen A40-S100. Specimen A40-S50 obtained 7.8% and 58.8% higher maximum axial load and ductility, respectively, compared to Specimen A40-S200. Also, Specimen A40-S50 obtained about 15.1% and 68.8% higher maximum axial load and ductility, respectively, compared to Specimen A40-S400. For

387 the increase of the spacing of lateral ties from 50 mm (1.96 in.) to 400 mm (15.74 in.), the maximum
388 axial load and ductility of the specimens reinforced with A40 SEA sections decreased by about
389 15.1% and 68.8%, respectively. These decreases in the strength and ductility of specimens reinforced
390 with A40 SEA were because the confinement of the concrete core decreased due to the increased
391 spacing of lateral tie up to 400 mm (15.74 in.). Under axial compression, the effect of lateral ties to
392 restrain the expansion of concrete core decreases as the spacing of lateral ties increases, which results
393 in decreasing the strength and ductility of the column, similar to specimens reinforced with
394 conventional steel bars.
395

396 ## EVALUATION OF CONCENTRIC AXIAL LOAD CAPACITY

397 The axial load capacity (P_n) for each column specimen was calculated using AS 3600-09[32] (Eq. (2)).
398 It is noted that the recommendation in AS 3600-09[32] is only applicable for conventional steel bar
399 reinforced concrete. In this study, Eq. (2) was used to calculate the axial load capacity for column
400 specimens reinforced longitudinally with SEA sections to investigate whether AS 3600-09[32] based
401 recommendations for steel bar reinforced concrete columns can be applied for the SEA reinforced
402 concrete columns.

$$P_n = \alpha_1 f_c' (A_g - A_s) + f_y A_s \quad (2)$$

403 where, A_g is the gross cross-sectional area of concrete column specimen, A_s is the total area of
404 longitudinal reinforcement, f_c' is the concrete compressive strength and f_y is the yield tensile strength
405 of longitudinal reinforcement. The α_1 is a reduction factor that takes into account the differences in
406 shape, concrete casting practice and size between standard concrete cylinders and concrete columns.
407 [35] In this study, the reduction factor is calculated according to AS 3600-09[32] as a function of the
408 compressive strength of concrete ($\alpha_1 = 1 - 0.003 f_c'$ within the limit $0.72 \leq \alpha_1 \leq 0.85$)
409 The experimental and calculated maximum axial loads of the tested column specimens are presented
410 in **Table 4**. In **Table 4**, P_{max} indicates the maximum axial load obtained from the experimental

investigations, P_n indicates the calculated axial load capacity using Eq. (2), and P_{max}/P_n indicates the ratio of the experimental to the calculated maximum axial load. It is noted that the spacing of lateral ties in Specimen B-S400 was much higher than the required spacing of lateral ties by ACI 318-14.[33]

It can be observed from **Table 4** that the P_{max}/P_n ratios are either higher than or equal to 1.0 when the lateral tie spacing is 50 mm (1.96 in.) and 100 mm (3.93 in.) for specimens reinforced with N12 steel bars and SEA sections. For the lateral tie spacing of 200 mm (7.87 in.) and 400 mm (15.74 in.), the P_{max}/P_n ratios are 0.91 and 0.65, respectively, for specimens reinforced with N12 steel bars. The rapid decrease of the P_{max}/P_n ratio for specimens reinforced with N12 steel bar indicates the loss of confinement effectiveness of the concrete core and the loss of buckling load of the steel bars for larger spacing of lateral ties. However, for the lateral tie spacing of 200 mm (7.87 in.) and 400 mm (15.74 in.), the P_{max}/P_n ratios are 0.97 and 0.96, respectively, for specimens reinforced with A30 SEA sections. Also, for the lateral tie spacing of 200 mm (7.87 in.) and 400 mm (15.74 in.), the P_{max}/P_n ratios are 0.98 and 0.92, respectively, for specimens reinforced with A40 SEA sections. The higher P_{max}/P_n ratios for specimens reinforced with SEA sections, especially for spacing of larger ties (200 mm (7.87 in.) and 400 mm (15.74 in.)), indicates the better performance of the specimens reinforced with A30 and A40 SEA sections compared to the specimens reinforced with N12 steel bars. Hence, larger lateral tie spacing might be recommended for specimens reinforced with A30 and A40 SEA sections.

CONCLUSIONS

Twelve square HSC column specimens were tested under concentric axial loads. Eight of the specimens were reinforced longitudinally with SEA sections (A30 and A40) to investigate the effect of the SEA sections as longitudinal reinforcement with different spacing of lateral ties. For comparison purposes, four specimens were reinforced longitudinally with conventional steel bars (N12 steel bars). Based on the test results of this study, the following conclusions are drawn:

1. In general, the failure of the specimens reinforced with N12 steel bars was characterised by the buckling of longitudinal bars, which was followed by the fracture of lateral ties at welded points for 50 mm (1.96 in.) and 100 mm (3.93 in.) center-to-center spacing of lateral ties. However, for 200 mm (7.87 in.) and 400 mm (15.74 in.) center-to-center spacing of lateral ties, the failure of the specimen was characterised by buckling of longitudinal steel bars and the crushing of concrete core. The failure of specimens reinforced with A30 and A40 SEA sections was characterized by the buckling of longitudinal SEA sections, which was followed by the fracture of lateral ties at welded points for 50 mm (1.96 in.) center-to-center spacing of lateral ties. Whereas, in general, the failure of specimens reinforced with A30 and A40 SEA sections with center-to-center spacing of lateral ties of 100 mm (3.93 in.) to 400 mm (15.74 in.) was attributed to the buckling of longitudinal SEA sections and then cracking of the concrete core.

2. The maximum axial loads of Specimens B-S50 and B-S100 were 11.6% and 2.7%, respectively, greater than the maximum axial loads of Specimens A30-S50 and A30-S100. However, at the maximum axial load, the force contribution of N12 steel bars in Specimen B-S50 and B-S100 was 27% higher than the force contribution of A30 SEA sections in Specimens A30-S50 and A30-S100, respectively. The maximum axial loads of Specimens B-S200 and B-S400 were 2.5% and 52%, respectively, lower than the maximum axial loads of Specimens A30-S200 and A30-S400. At the same lateral tie spacing, all specimens reinforced with A30 SEA sections exhibited higher ductility compared to reference specimens reinforced with N12 steel bars. This was because the use of the A30 SEA sections as longitudinal reinforcement in HSC column specimens increased the effective confinement of the concrete core of the specimens.

3. For the same center-to-center spacing of lateral ties, all specimens reinforced longitudinally with A40 SEA sections exhibited higher maximum axial load and ductility than the corresponding specimens reinforced longitudinally with N12 steel bars. Increasing the spacing of lateral ties from 50 mm (1.96 in.) to 400 mm (15.74 in.) led to a decrease of 15.1% of the maximum axial load for specimens reinforced with A40 SEA sections. In addition, Specimens A40-S50, A40-S100, and A40-

S200 showed higher maximum axial load and ductility compared to the Specimens A30-S50, A30-S100 and A30-S200, respectively. The reason for higher maximum axial load and ductility of specimens reinforced with A40 SEA sections was due to the combined effect of the increased confinement effectiveness of the concrete core and the greater cross section area of A40 SEA section 4. For the same center-to-center spacing of lateral ties, all specimens reinforced longitudinally with A40 SEA sections exhibited higher maximum axial load and ductility than the corresponding specimens reinforced longitudinally with N12 steel bars. Increasing the spacing of lateral ties from 50 mm (1.96 in.) to 400 mm (15.74 in.) led to a decrease of 15.1% of the maximum axial load for specimens reinforced with A40 SEA sections. In addition, Specimens A40-S50, A40-S100, and A40-S200 showed higher maximum axial load and ductility compared to the Specimens A30-S50, A30-S100 and A30-S200, respectively. The reason for higher maximum axial load and ductility of specimens reinforced with A40 SEA sections was due to the combined effect of the increased confinement effectiveness of the concrete core and the greater cross section area of A40 SEA section 5. For specimens with lateral tie spacing of 400 mm (15.74 in.), the use of the conventional steel bar as longitudinal reinforcement led to a premature failure of the specimen, while the use of the SEA sections as longitudinal reinforcement did not lead to premature failure of the specimen. This was because the buckling load of SEA sections was significantly higher than the buckling load of steel bars.

Finally, based on the test results of the HSC column specimens, it is evident that the use of SEA sections as longitudinal reinforcement for HSC columns can provide higher maximum axial load and ductility compared to the HSC columns reinforced longitudinally with conventional steel bars.

ACKNOWLEDGMENTS

The authors would like to thank the University of Wollongong, Australia and technical officers at the High Bay laboratory for their help in the experimental program of this study. Also, the first author thanks the support of the Iraqi Government for his full Ph.D. scholarship.

REFERENCES

1. Mirza, S. A., Hyttinen, V., and Hyttinen, E., "Physical Tests and Analyses of Composite Steel-Concrete Beam-Columns," *Journal of Structural Engineering*, ASCE, V. 122, No. 11. 1996, pp. 1317-1326.

2. Ellobody, E., and Young, B., "Numerical Simulation of Concrete Encased Steel Composite Columns," *Journal of Constructional Steel Research*, V. 67, No. 2. 2011, pp. 211-222.

3. Kim, C. S., Park, H. G., Chung, K. S., and Choi, I. R., "Eccentric Axial Load Testing for Concrete-Encased Steel Columns Using 800 MPa Steel and 100 MPa Concrete," *Journal of Structural Engineering*, ASCE, V. 138, No. 8. 2012, pp. 1019-1031.

4. Hunaiti, Y., Fattah, B. A., and Fattah, A., "Design Considerations of Partially Encased Composite Columns," *Proceedings of the ICE-Structures and Buildings*, V. 104, No. 1. 1994, pp. 75-82.

5. Leite, L., Bonet, J., Pallarés, L., Miguel, P. F., and Fernández-Prada, M. A., "Experimental Research on High Strength Concrete Slender Columns Subjected to Compression and Uniaxial Bending with Unequal Eccentricities at the Ends," *Engineering Structures*, V. 48, 2013, pp. 220-232.

6. Campione, G., Monaco, A., and Minafò, G., "Shear Strength of High-Strength Concrete Beams: Modeling and Design Recommendations," *Engineering Structures*, V. 69, 2014, pp. 116-122.

7. Hadi, M. N. S., Balanji, E. K., and Sheikh, M. N., "Behavior of Steel Fiber-Reinforced High-Strength Concrete Columns under Different Loads," *ACI Structural Journal*, V. 114, No. 04. 2017, pp. 815-826.

8. Sheikh, S. A., Shah, D. V., and Khoury, S. S., "Confinement of High-Strength Concrete Columns," *ACI Structural Journal*, V. 91, No. 1. 1994, pp. 100-111.

9. El-Tawil, S., and Deierlein, G. G., "Strength and Ductility of Concrete Encased Composite Columns," *Journal of Structural Engineering*, V. 125, No. 9. 1999, pp. 1009-1019.

10. Li, B., and Park, R., "Confining Reinforcement for High Strength Concrete Columns," *ACI Structural Journal*, V. 101, No. 3. 2004, pp. 314-324.

514 11. Ho, J., Lam, J., and Kwan, A., "Effectiveness of Adding Confinement for Ductility Improvement
515 of High-Strength Concrete Columns," *Engineering Structures*, V. 32, No. 3. 2010, pp. 714-725.
516 12. Awati, M., and Khadiranaikar, R., "Behavior of Concentrically Loaded High Performance
517 Concrete Tied Columns," *Engineering Structures*, V. 37, . 2012, pp. 76-87.
518 13. Woods, J. M., Kiousis, P. D., Ehsani, M. R., Saadatmanesh H., and Fritz W., "Bending Ductility
519 of Rectangular High Strength Concrete Columns," *Engineering structures*, V. 29, No. 8. 2007, pp.
520 1783-1790.
521 14. Samani, A. K., Attard, M. M., and Foster, S. J., "Ductility in Concentrically Loaded Reinforced
522 Concrete Columns," *Australian Journal of Structural Engineering*, V. 16, No. 3. 2015, pp. 237-250.
523 15. Yang, K. H., and Kim, W. W., "Axial Compression Performance of Reinforced Concrete Short
524 Columns with Supplementary V-Shaped Ties," *ACI Structural Journal*, V. 113, No. 6. 2016, pp.
525 1347-1356.
526 16. Razvi, S. R., and Saatcioglu, M., "Strength and Deformability of Confined High-Strength
527 Concrete Columns," *ACI Structural Journal*, V. 91, No. 6. 1994, pp. 678-687.
528 17. Shin, H. O., Yoon, Y. S., Cook, W. D., and Mitchell, D., "Enhancing the Confinement of Ultra-
529 High-Strength Concrete Columns Using Headed Crossties," *Engineering structures*, V. 127, 2016,
530 pp. 86-100.
531 18. Foster, S. J., "Design and Detailing of High Strength Concrete Columns," UNICIV Report No.
532 R-375, University of New South Wales, Sydney, Australia, 1999.
533 19. Popovic, D., Hancock, G. J., and Rasmussen, K. J. R. (1999). "Axial compression tests of cold-
534 formed angles." *Journal of Structural Engineering*. V. 125, No. 5, pp. 515-523.
535 20. Young, B. (2004). "Tests and design of fixed-ended cold-formed steel plain angle columns."
536 Journal of structural engineering. V. 130, No. 12, pp. 1931-1940.
537 21. Ellobody, E., and Young, B. (2005). "Behavior of cold-formed steel plain angle columns."
538 *Journal of structural engineering*. V. 131, No. 3, pp. 457-466.

539 22. AS 1012.3.1-14, "Methods of testing concrete—Method 3.1: determination of properties related
540 to the consistency of concrete—Slump test." Standards Australia, Sydney, Australia, 2014.
541 23. AS 1012.9-99, "Methods of Testing Concrete, Determination of the Compressive Strength of
542 Concrete Specimens," Standard Australia, Sydney, Australia, 1999
543 24. AS 1391-07,“Metallic Materials-Tensile Testing at Ambient Temperature,” Standards Australia,
544 Sydney, Australia, 2007.
545 25. OneSteel, "Know Your Steel: Steel Reference Guide,", 2010, [www.onesteel.com].
546 26. Hadi, M. N. S., and Youssef, J., "Experimental Investigation of GFRP-Reinforced and GFRP-
547 Encased Square Concrete Specimens under Axial and Eccentric Load, and Four-Point Bending Test,"
548 *Journal of Composites for Construction*, ASCE, V. 93, 2016, pp. 1-16.
549 27. Hadi, M. N. S., Khan, Q. S., and Sheikh, M. N., "Axial and Flexural Behavior of Unreinforced
550 and FRP Bar Reinforced Circular Concrete Filled FRP Tube Columns," *Construction and Building*
551 *Materials*, V. 122, 2016, pp. 43-53.
552 28. Pessiki, S., and Pieroni, A., "Axial Load Behavior of Large-Scale Spirally-Reinforced High-
553 Strength Concrete Columns," *ACI Structural Journal*, V. 94, No. 3. May-June 1997, pp. 304-313.
554 29. Sheikh, M. N., and Legeron, F., "Performance Based Seismic Assessment of Bridges Designed
555 According to Canadian Highway Bridge Design Code," *Canadian Journal of Civil Engineering*, V.
556 41, No. 9. 2014, pp. 777-787.
557 30. Mander, J. B., Priestley, M. J., and Park, R. (1988). "Theoretical stress-strain model for
558 confined concrete." *Journal of Structural Engineering.* V. 114, No. 8, 1988, pp. 1804-1826.
559 31. Campione, G., and Minafò, G., "Compressive Behavior of Short High-Strength Concrete
560 Columns," *Engineering Structures*, V. 32, No. 9. 2010, pp. 2755-2766.
561 32. AS 3600-09, “Concrete Structures,” Standards Australia, Sydney, Australia, 2009.
562 33. ACI Committee 318, “Building Code Requirements for Structural Concrete (ACI 318-14) and
563 Commentary,” American Concrete Institute, Farmington Hills, MI, 2014, 148 pp.

34. Saatcioglu, M., and Razvi, S. R., "High-Strength Concrete Columns with Square Sections under Concentric Compression," *Journal of Structural Engineering*, ASCE, V. 124, No. 12. 1998, pp. 1438-1447.

35. Ozbakkaloglu, T., and Saatcioglu, M., "Rectangular Stress Block for High-Strength Concrete," *ACI Structural Journal*, V. 101, No. 4. 2004, pp. 475-483.

TABLES AND FIGURES

List of Tables:

List of Figures:

Table 1–Test matrix

Group	Specimen Labels	Longitudinal Reinforcement						Lateral Reinforcement	
		Reinforcement Type	Number	Bar		Steel Equal Angle (SEA) Section			
				Diameter (mm)	ρ_b %	Dimension (mm)	ρ_{SEA} %	Diameter (mm)	Spacing (mm)
B	B-S50	Steel Bar	4	12	1.03	-	-	10	50
	B-S100								100
	B-S200								200
	B-S400								400
A30	A30-S50	Steel Equal Angle (SEA) Section	4	-		29.1 × 2.25	1.11	10	50
	A30-S100								100
	A30-S200								200
	A30-S400								400
A40	A40-S50	Steel Equal Angle (SEA) Section	4	-		39.3 × 3.7	2.43	10	50
	A40-S100								100
	A40-S200								200
	A40-S400								400

Notes: 1 mm = 0.0393 in.

ρ_b Volumetric ratio of longitudinal reinforcement (steel bars) in specimen cross section.

ρ_{SEA} Volumetric ratio of longitudinal reinforcement (steel equal angle sections) in specimen cross section.

Table 2–Tensile properties of steel equal angle (SEA) sections

Steel Equal Angle (SEA)Section	Leg Width (mm)	Thickness (mm)	Area (mm^2)	Yield Tensile Strength (MPa)	Modulus of Elasticity (GPa)
Nominal					
A30	30	2.5	132	350	200
A40	40	4	280	450	200
Measured (average)					
A30	29.1	2.25	122.6	374	208
A40	39.3	3.7	268.3	473	205

Notes: 1 mm = 0.0393 in.; 1 MPa = 0.1450 ksi.

Table 3–Summary of the test results of column specimens

Specimen	Maximum concentric axial load, P_{max} (kN)	Axial deformation at P_{max} (mm)	Ultimate Axial Deformation Δ_u [a] (mm)	Ductility
B-S50	2929	2.3	3.1	1.8
A30-S50	2625	2.2	4.0	2.6
A40-S50	3009	2.2	3.9	2.7
B-S100	2626	2.1	2.7	1.6
A30-S100	2619	2.3	2.8	1.8
A40-S100	2836	2.4	3.2	1.9
B-S200	2399	1.8	2.3	1.5
A30-S200	2469	1.9	2.4	1.6
A40-S200	2791	2.2	2.8	1.7
B-S400	1717	1.8	-	-
A30-S400	2446	2.1	2.4	1.5
A40-S400	2614	2.2	2.7	1.6

Notes: 1 kN = 0.2248 kip; 1 mm = 0.0393 in.

[a] represents the deformation corresponding to 80% of the maximum axial load in the descending branch of the axial load-axial deformation behavior.

Table 4 – Experimental and analytical concentric axial load capacity of column specimens

Group	Specimen	Maximum concentric axial load (kN)		$\frac{P_{max}}{P_n}$
		Experimental (P_{max})	Analytical (P_n)	
B	B-S50	2929	2627	1.11
	B-S100	2626	2627	1.00
	B-S200	2399	2627	0.91
	B-S400	1718	2627	0.65
A30	A30-S50	2625	2557	1.03
	A30-S100	2619	2557	1.02
	A30-S200	2469	2557	0.97
	A30-S400	2446	2557	0.96
A40	A40-S50	3009	2849	1.06
	A40-S100	2836	2849	1.00
	A40-S200	2791	2849	0.98
	A40-S400	2614	2849	0.92

Note: 1 kN = 0.2248 kip

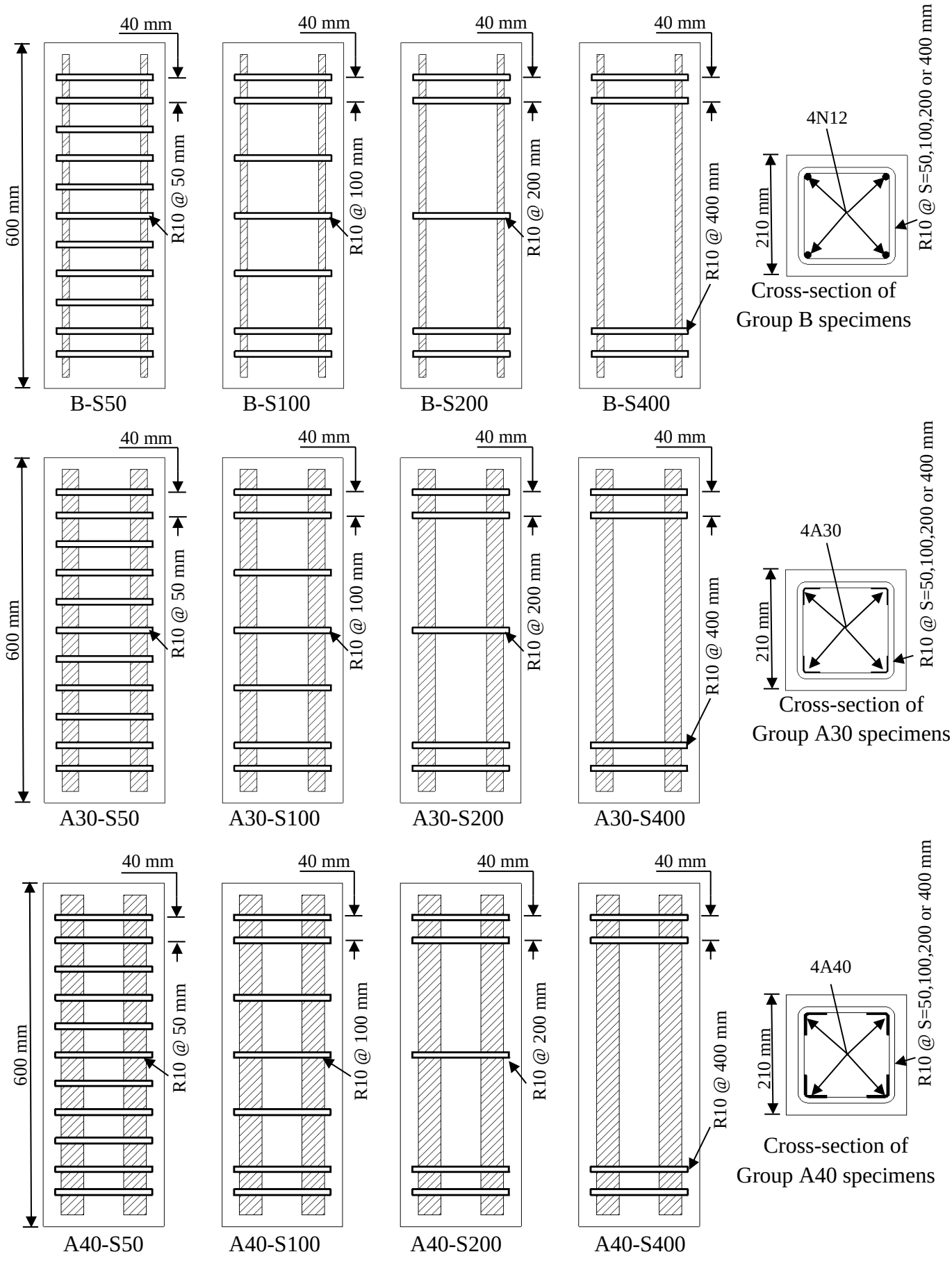

Fig. 1–Geometry and reinforcement details of the column specimens. *(Note: 1 mm = 0.0393 in.)*

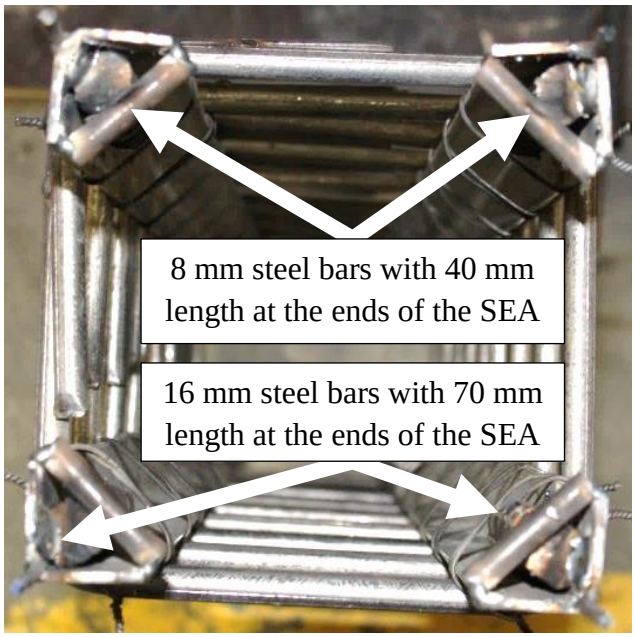

Fig. 2–Steel cage with SEA sections. *(Note: 1 mm = 0.0393 in.)*

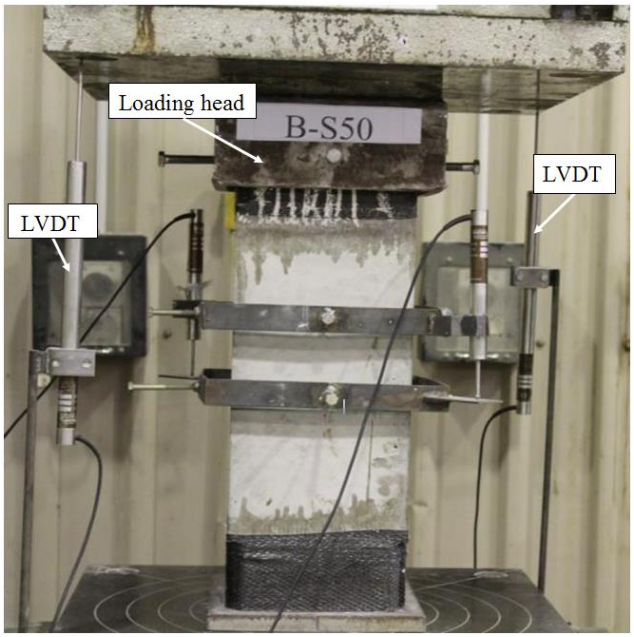

Fig. 3–Test setup.

B-S50 B-S100 B-S200 B-S400

(a)

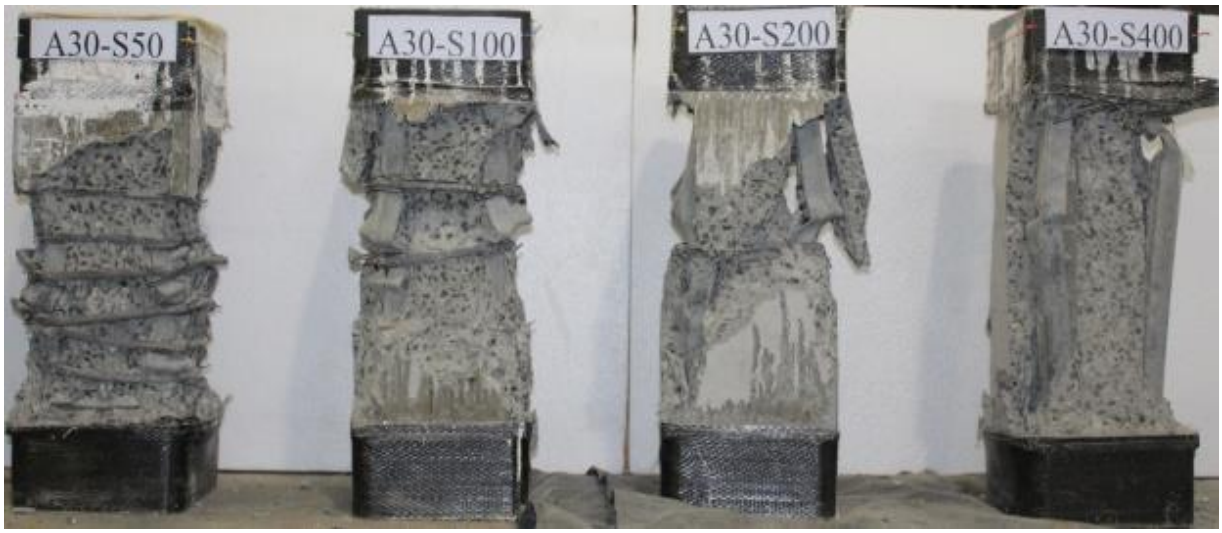

A30-S50 A30-S100 A30-S200 A30-S400

(b)

A40-S50 A40-S100 A40-S200 A40-S400

(c)

Fig. 4–Tested specimens after failure: (a) Group B Specimens, (b) Group A30 specimens; and (c) Group A40 specimens.

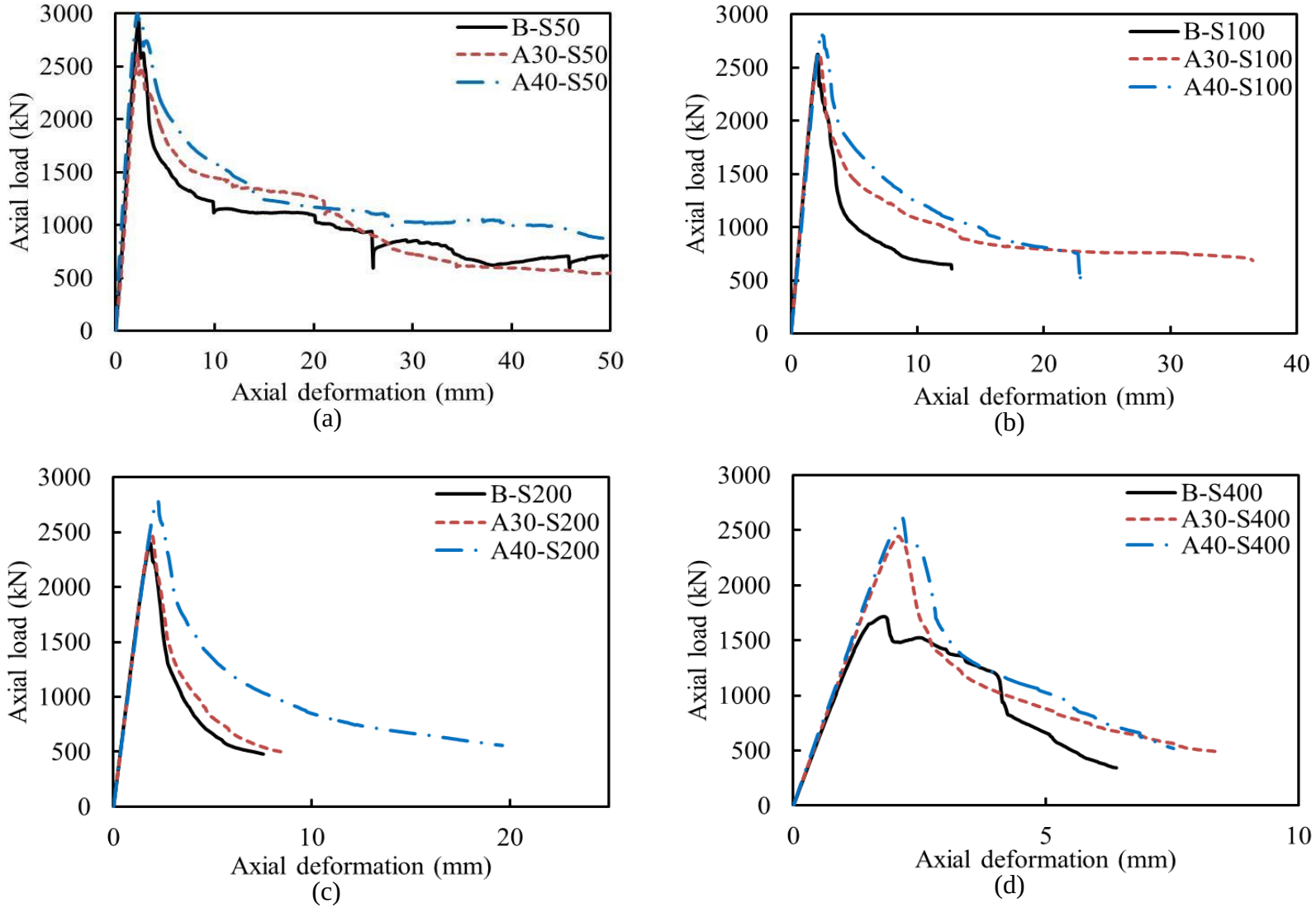

Fig. 5–Axial load-axial deformation response of column specimens with tie spacing: (a) 50 mm; (b) 100 mm; (c) 200 mm; and (d) 400 mm.

(Note: 1 kN =0.2248 kip; 1 mm = 0.0393 in.)

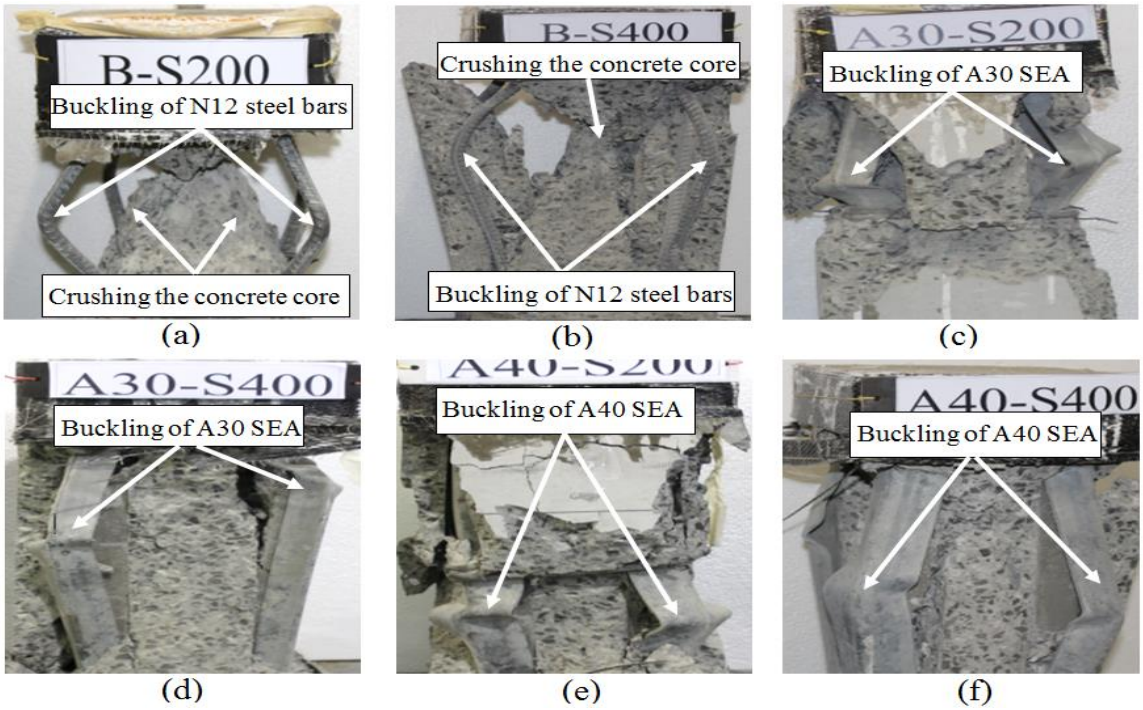

Fig. 6–Close-up views of the failure modes of column specimens (a) B-S200; (b) B-S400; (c) A30-S200; (d) A30-S400; (e) A40-S200; and (f) A40-S400.

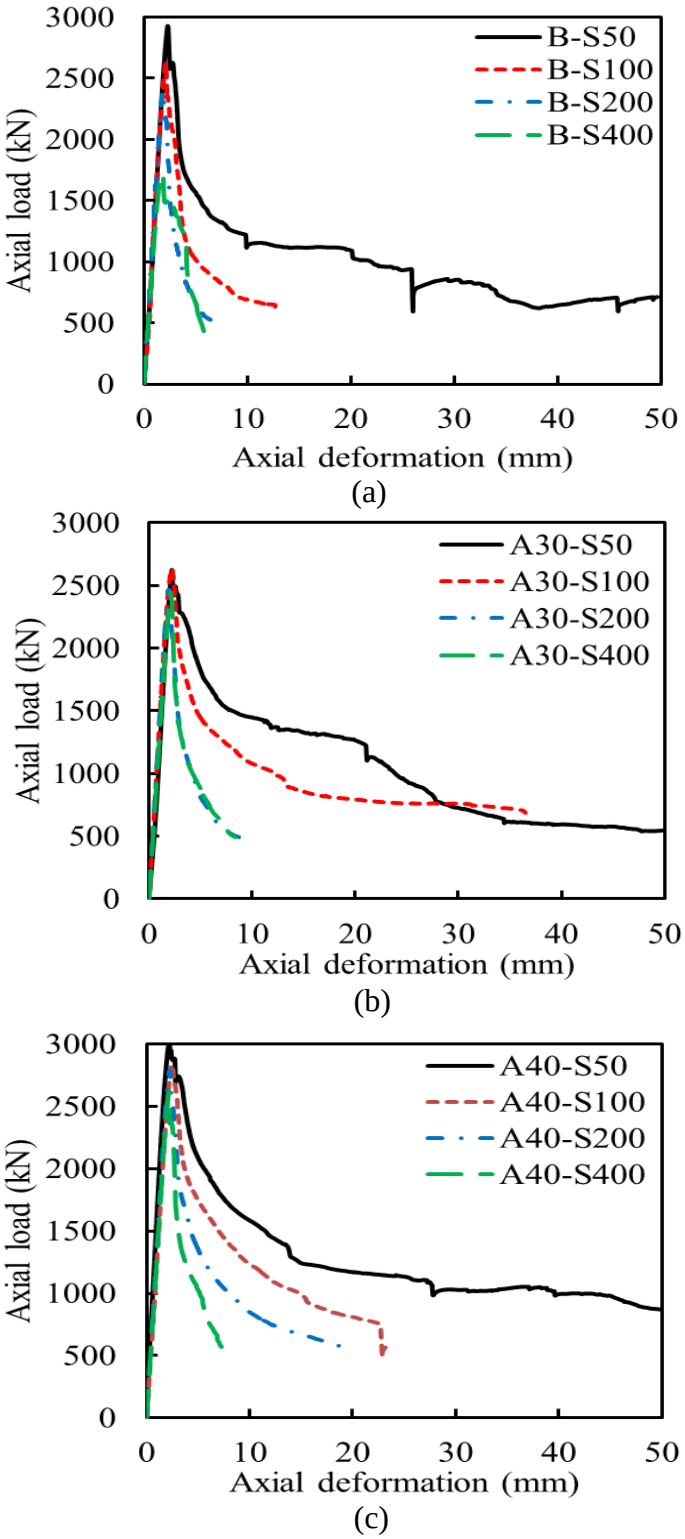

Fig. 7–Axial load-axial deformation response: (a) Group B specimens; (b) Group A30 specimens; and (c) Group A40 specimens. *(Note: 1 kN =0.2248 kip; 1 mm = 0.0393 in.)*